

A first principle investigation of the polarized evanescent d states in Co/SrTiO₃ magnetic junctions

This article has been downloaded from IOPscience. Please scroll down to see the full text article.

2004 J. Phys.: Condens. Matter 16 1603

(<http://iopscience.iop.org/0953-8984/16/9/008>)

View [the table of contents for this issue](#), or go to the [journal homepage](#) for more

Download details:

IP Address: 171.66.16.179

The article was downloaded on 13/05/2010 at 11:24

Please note that [terms and conditions apply](#).

A first principle investigation of the polarized evanescent d states in Co/SrTiO₃ magnetic junctions

Daniel Stoeffler

Institut de Physique et de Chimie des Matériaux de Strasbourg (UMR C7504 CNRS-ULP),
23 rue du Loess, BP 43, F-67034 Strasbourg, France

E-mail: Daniel.Stoeffler@ipcms.u-strasbg.fr

Received 27 June 2003

Published 20 February 2004

Online at stacks.iop.org/JPhysCM/16/1603 (DOI: 10.1088/0953-8984/16/9/008)

Abstract

The band structure of SrO terminated Co/SrTiO₃ superlattices is investigated within the first principle augmented spherical wave method allowing us to discuss the oxide induced polarization and to examine the decay of the evanescent states into the oxide layer which is essential for the understanding of tunnelling phenomena through the insulator. The calculated d polarization of the Co electrode at the interface confirms qualitatively the interpretation of the measurements and presents a crossover from positive to negative values around $E_F - 0.9$ eV. It is also shown that, due to the high d character of the band structure of Sr and Ti, d states do not decay more rapidly into the oxide layer than s or p states, and they have a preserved polarization.

Spin polarized tunnelling in magnetic tunnel junctions (MTJ) is of renewed interest due to the measurement of large tunnel magnetoresistance (TMR) values for various metal/oxide/metal trilayers [1]. If recent elaboration progress has allowed the growth of well defined insulator barriers and offers promising potential applications of MTJ in the domains of magnetic sensors or magnetic random access memories, they also allow us to investigate fundamental aspects of the tunnelling through thin oxide layers such as the electronic structure of interfaces [2], rare events phenomena [3, 4], and micromagnetic structure of the electrodes [5]. Recently, crystalline SrTiO₃ [2] and MgO [6] layers in MTJ have been grown which, unlike Al₂O₃ based MTJ, are good candidates for direct comparison with realistic theoretical band structure calculations [7, 8].

Usually, the TMR is analysed in terms of the metallic magnetic electrode (M_i) tunnelling spin polarization (P_i) using Jullière's model [9] giving

$$\text{TMR} = \frac{2P_1 P_2}{1 + P_1 P_2} \quad \text{with } P_i = \frac{D_i^\uparrow(E_F) - D_i^\downarrow(E_F)}{D_i^\uparrow(E_F) + D_i^\downarrow(E_F)} \quad (1)$$

where $D_i^\sigma(E_F)$ is the tunnelling density of states (TDOS) of electrode M_i for spin σ at the Fermi level E_F . A crude approximation consists of using the integrated DOS $n_i^\sigma(E_F)$ assuming that all states are identically attenuated into the oxide barrier. The approximated polarization is then taken equal to

$$\tilde{P}_i = \frac{n_i^\uparrow(E_F) - n_i^\downarrow(E_F)}{n_i^\uparrow(E_F) + n_i^\downarrow(E_F)}. \quad (2)$$

For example, this approach has been used to interpret the occurrence of inverse TMR in Co/SrTiO₃/LSMO trilayers for an applied bias voltage V larger than +0.8 eV [2]. Another approximation made in this interpretation is the use of a DOS taken from a Co/vacuum interface which does not take into account the hybridization between metallic and oxide states, whereas recent theoretical works have shown that this hybridization can significantly affect the electronic structure at the interface [7, 8].

It has also been shown that, for such epitaxial metal/oxide junctions where the oxide layer is crystalline, a k_{\parallel} analysis has to be done in order to identify the k_{\parallel} -states presenting the slowest decay in the barrier and having the main contribution to the tunnelling. In the asymptotic regime, where the thickness of the oxide can be assumed as being infinite, these k_{\parallel} -states correspond to the ones where the imaginary part of k_{\perp} , taken from the complex bulk-like bands $E(k_{\parallel}, k_{\perp})$ of the SrTiO₃ oxide, is the smallest [10]. This will select a few interfacial Co states, having these particular k_{\parallel} vectors, that couple with these slowly decaying k_{\parallel} -states. Consequently, the TMR results from contributions of a limited number of spin-polarized Co states rather than \mathbf{k} integrated quantities like the DOS. This restricts the use of the Jullière model with $n_i^\sigma(E_F)$ to the ‘dirty interface’ limit where all k_{\parallel} vectors contribute to the tunnelling because the k_{\parallel} conservation is lost at the interfacial boundaries.

In the present work, we determine the electronic structure at a Co/SrTiO₃ interface, with an SrO termination for the oxide layer, using the first principle augmented spherical wave method [11] in order to take into account the bonding between metal and oxide atoms, and we examine the characteristics of the evanescent states.

The unit cell is built by matching an FCC(001) Co layer consisting of 5 atomic layers to a bulk-like SrTiO₃ oxide layer consisting of 13 atomic layers of alternating SrO and TiO₂ planes terminated by SrO planes in the fourfold hollow adsorption sites. This termination has been chosen because the orbital overlap at the interfaces is small and does not introduce too extended perturbations into the Co and the oxide electronic structure contrary to what is obtained with the TiO₂ termination [8]; this allows us to identify more easily the asymptotic features and to recover bulk-like electronic structure at the centre of the oxide even with a relatively thin oxide layer. As a first step and because we remain at a qualitative level of discussion, atomic relaxation at the metal/oxide interface is not taken into account. The matching between the Co and the oxide layers is obtained by imposing the same in-plane square cell to all layers and by compressing the Co layer in the perpendicular direction in order to conserve the atomic volume of the Co atoms. A previous work [8] has shown that the relaxed structure is not very different from the one built with this approximation. With such an approach, the denser TiO₂ termination leads to unphysical sphere overlaps introducing unphysical shifted levels to energies below the bottom of the oxide valence band.

Before examining the electronic structure of the Co/SrTiO₃ superlattice, let us discuss briefly the bulk band structure of SrTiO₃ displayed in figure 1. Within the local density approximation (LDA), the conduction band is found too low in energy by approximately 1.5 eV and the indirect gap energy E_g is found equal to 2.0 eV. This underestimation is usual in LDA calculations because only single-electron states are considered. Our result is in very good agreement with previous LDA calculations giving $E_g = 1.9$ eV [12]. The s, p and d

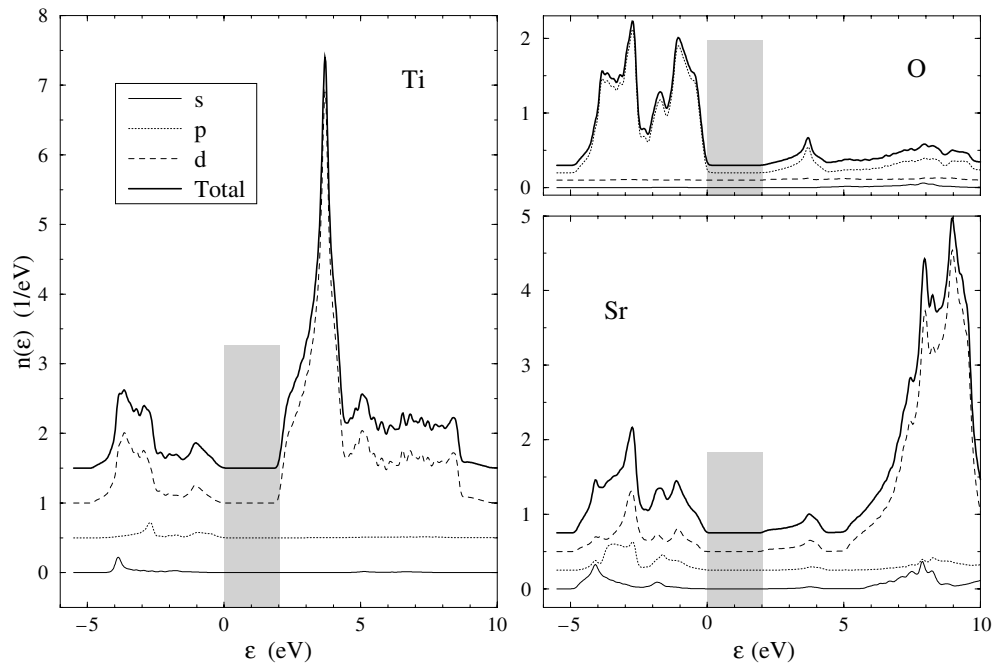


Figure 1. Site and symmetry projected densities of states of bulk SrTiO₃. The grey domain corresponds to the energy gap. For clarity, the curves have been offset and the zero of energy of each curve can be obtained by using its value into the gap domain.

symmetries projected densities of states (DOS) show clearly that, in accordance with the atomic configuration of the valence states, i.e. $2p^4$ for O, $3d^2$ for Ti and $5s^23d^0$ for Sr,

- (i) only p states are present on the O site,
- (ii) d states corresponds to nearly all states on the Ti site with a weak hybridization with s and p states in the valence band, and
- (iii) s, p and d states are strongly hybridized in the valence band of Sr and the dominant d states are weakly hybridized with s and p states in the conduction band of the Sr site.

This result shows that d states are highly represented on each (001) atomic layer in the SrTiO₃ crystal, suggesting a significant hybridization of these states with the metal ones in the Co/SrTiO₃ MTJ.

The site projected DOS around the metal/oxide interface of the Co/SrTiO₃ superlattice are displayed in figure 2, and the local magnetic moments and charges are given in table 1. In order to compare to the band structure of the equivalent surface, the site projected DOS for a 5 atomic layers thick slab are given in figure 3. For the calculation of the electronic structure of the slab, 5 atomic layers of empty spheres have been included playing the role of the vacuum. From a general point of view, the DOS on the three inequivalent Co sites for both systems are very similar: the main difference comes from more pronounced peaks in the DOS for the slab. The DOS on the central Co atomic layer are very similar to the one of bulk body centred tetragonal (BCT) Co exhibiting a pronounced valley around their middle and showing that bulk properties are recovered in the centre of our 5 atomic layer thick Co layer. As expected, the most significant differences between the slab and the multilayer are obtained for the interfacial or the surface atomic layer. The middle valley in the surface DOS

Table 1. Local moment and local charge on the inequivalent sites of the Co layer and on the first two atomic layers (C refers to central and I to interfacial) of the SrTiO₃ oxide layer in the Co/SrTiO₃ multilayer.

	Local moment (μ_B)	Local charge (e)
Co (C)	1.71	0.01
Co	1.61	0.09
Co (I)	1.65	-0.33
Sr (I)	0.05	0.70
O (I)	0.11	0.31
Ti (I + 1)	<0.01	-2.13
O (I + 1)	<0.01	0.51

is nearly filled by two supplementary peaks that are due to the surface state of the d_z^2 orbital pointing out of the surface. The comparison with the interfacial Co DOS obtained by Oleinik and co-workers [8] shows a surprisingly good agreement with the present one. This results from the fact that, even if the interfacial bonding between the oxide and the Co atoms is much stronger than in the present case, their interfacial oxide states are pushed to lower energy values and the interfacial hybridization is strongly reduced. For the metal/oxide interface, similar but less pronounced peaks are obtained, indicating that the presence of the Sr and O atoms only slightly affects the orbitals of the Co atoms. Similarly, only the interfacial Co atoms exhibit a significant charge variation, inducing a slight increase of the local magnetic moment, and the total charge transfer from the metal to the oxide layer is found equal to 0.23 electrons per interfacial Co atom. All this charge is transferred on the interfacial atomic layer of the oxide and only the interfacial Sr and O atoms carry a significant local magnetic moment aligned parallel to the Co moment, contrary to what has been found for the TiO₂ termination [8]. When considering successive atomic planes from the interface to the centre of the oxide layer, the local DOS becomes very rapidly similar to the bulk ones, in agreement with the expected exponential decay of the evanescent wavefunction into the insulating barrier. To summarize, the DOS for both spins on the Co interfacial atomic layer are found to be not very different from surface DOS.

This calculation allows us now to discuss the polarization \tilde{P} as defined in equation (2) for a realistic Co DOS at the Co/SrTiO₃ interface in order to confirm the interpretation of the occurrence of inverse TMR in terms of the polarization of the d DOS [2]. The d polarization $\tilde{P}_d(\text{Co})$ (figure 4) is found to be nearly equal to -0.94 around E_F , giving a large negative TMR (inverse TMR) for an applied bias voltage V equal to zero. In agreement with [2], $P(\text{LSMO})$ is taken to be equal to 0.8 in the calculation of the TMR. For energies below -0.9 eV, $\tilde{P}_d(\text{Co})$ is positive and reaches a maximum of $+0.52$ around -1.1 eV. Consequently, even if the complete calculation of the TMR for $V \neq 0$ requires us to integrate all states between the ‘Fermi’ levels of both electrodes [13], we can expect a change of sign of the TMR for positive V . The comparison with the polarization \tilde{P} of the surface DOS shows only small differences around the Fermi level. This comes from the fact that the mostly different majority spin DOS at the metal/oxide interface exhibits peculiar structures for energies more than 1 eV below E_F , and plays no role on variations of the polarization \tilde{P} around E_F .

The comparison between the Co isolated slab and the same layer in Co/SrTiO₃ multilayers has shown that the interfacial hybridization affects the Co electronic structure very slightly. However, even if the induced states into the oxide gap are evanescent and have an exponential decay, the electronic structure of the whole oxide layer is highly affected by these induced states nearly filling the gap. The Fermi level E_F is pinned by the electron filling of these states, and depending on the nature of the interfacial hybridization, on the gap induced states and on

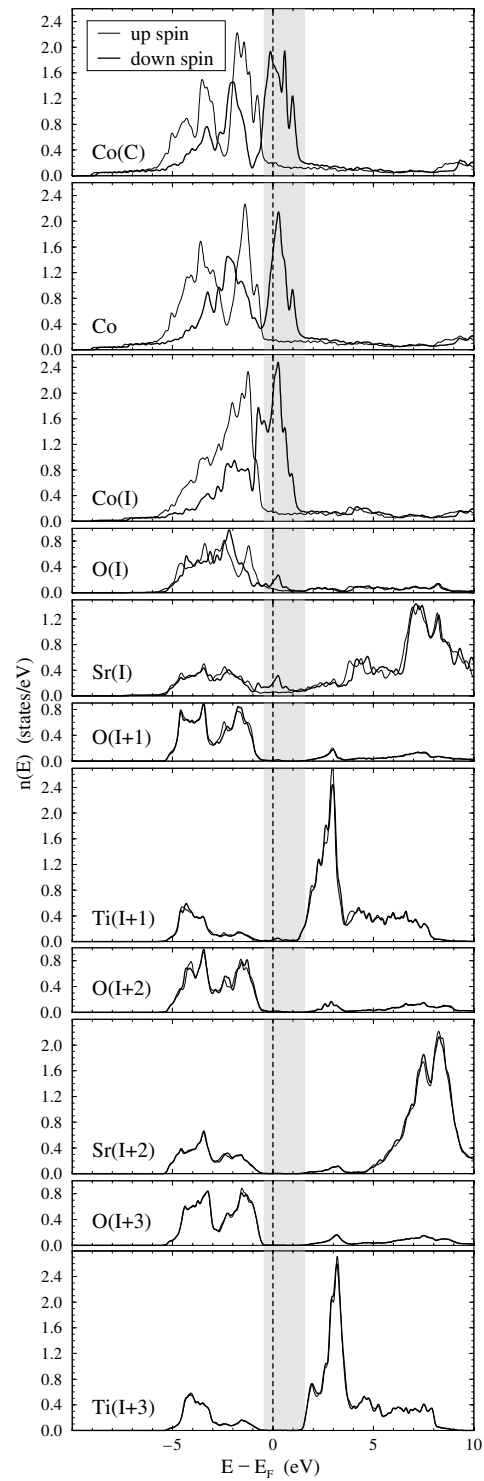


Figure 2. Site and spin projected densities of states on the inequivalent sites of the Co layer and on the first four atomic layers (C refers to central and I to interfacial) of the SrTiO₃ oxide layer in the Co/SrTiO₃ multilayer. The grey domain corresponds to the energy gap.

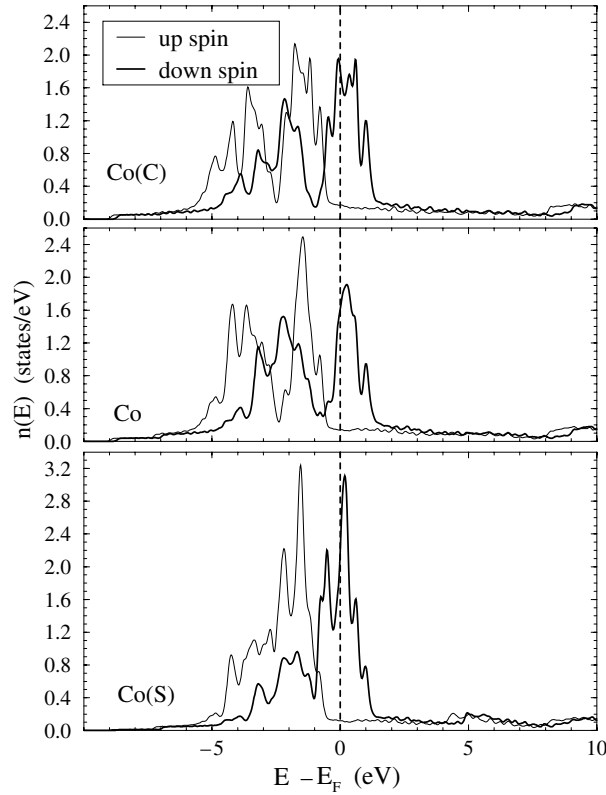


Figure 3. Site and spin projected densities of states on the inequivalent sites of the Co slab (C refers to central and S to surface).

the amount of electrons transferred from the metal to the oxide, the pinning can occur in a wide energy range of the oxide gap. This makes the Fermi level position into the gap, and all properties directly related to E_F , very sensitive to the nature of the interface. In the present work, an arbitrary Co/SrO interface has been built as illustration, and the discussion has to remain at a qualitative level.

The calculated TMR at zero applied voltage is found to be at least one order of magnitude larger than the experimental value [2]. This discrepancy comes *a priori* from the too crude approximation of a similar thickness decay for all evanescent states into the oxide layer and the use of $n_i^\sigma(E_F)$ in the Jullière model. For such epitaxial metal/oxide junctions where the oxide layer is crystalline, a k_{\parallel} analysis has to be done. It has been shown that the distribution into the two-dimensional Brillouin zone of the highly conducting k_{\parallel} -states is strongly sensitive to the oxide thickness, and that the states around the Γ point become predominant in most situations [14]. Consequently, we have to consider a realistic oxide thickness and, because a small thickness does not allow us to determine the decay length for each k_{\parallel} -wavefunction accurately, we have to focus on the dominant k_{\parallel} -states into the local DOS at the centre of the oxide layer. The last part of this paper is devoted to a k_{\parallel} analysis of the evanescent wavefunctions for the present oxide thickness (~ 2 nm), nearly corresponding to the experimental one (~ 2.5 nm) [2].

Figure 5 shows the distribution of the densities of states on the central SrTiO₃ oxide layers for both spins into the 1/8 irreducible part of the two-dimensional Brillouin zone. The two

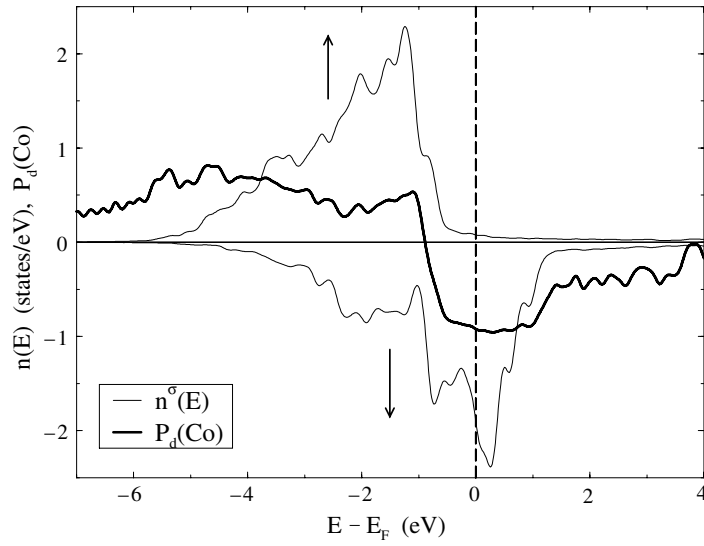


Figure 4. Spin projected d densities of states on the interfacial Co atomic layer (thin curve) and resulting d polarization $\bar{P}_d(\text{Co})$ (thick curve).

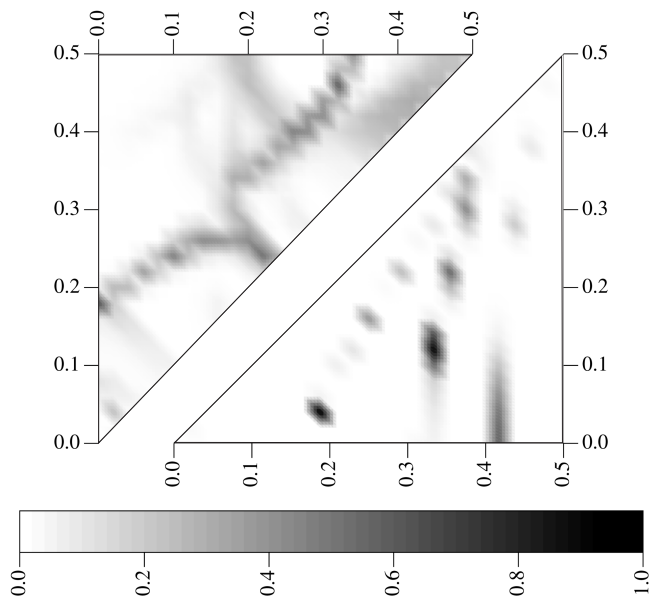


Figure 5. Distribution into the irreducible part of the two-dimensional Brillouin zone of the majority (lower triangle) and minority (upper triangle) spin density of states $n^\sigma(E_F, k_{\parallel})$ on the central SrTiO₃ layers. The k_x and k_y values are given in reduced units relative to $k_{x,\text{max}} = k_{y,\text{max}} = 2\pi/a$ where a is the in-plane lattice parameter, and the grey scale for $n^\sigma(E_F, k_{\parallel})$ is given relative to the maximum value $n^\uparrow(E_F, k_{\parallel} = (0.20, 0.04))$.

distributions display very different features: the majority spin distribution presents a small number of high value spots (dark in the figure), whereas the minority spin one presents a line (dark grey nearly parallel to the diagonal) of high value k_{\parallel} points. This dissimilar behaviour

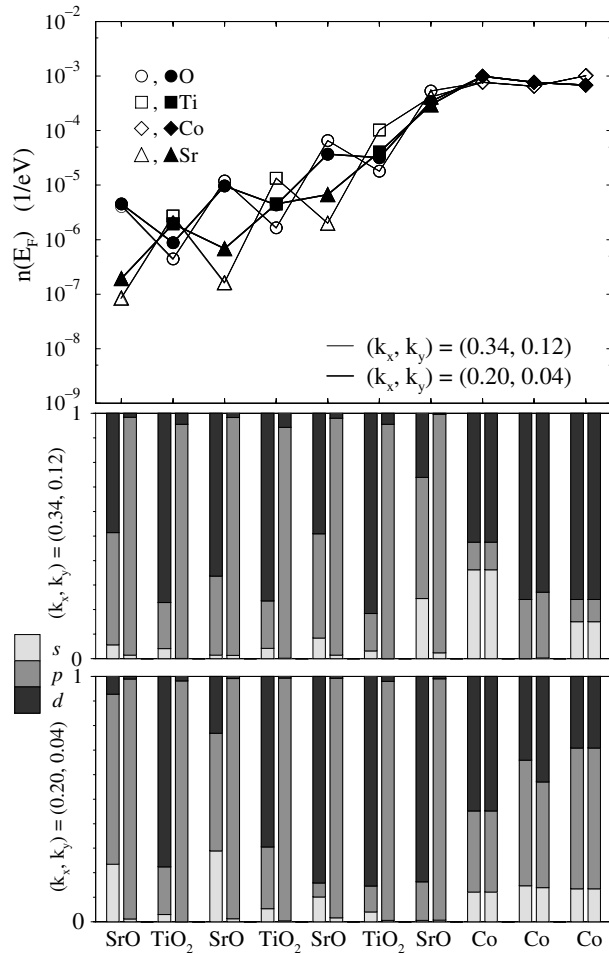


Figure 6. Top: k_{\parallel} projected majority spin density of states values $n^{\uparrow}(E_F, k_{\parallel})$ at the Fermi level E_F on each inequivalent layer of the Co/SrTiO₃ multilayer for $(k_x, k_y) = (0.34, 0.12)$ and $(0.20, 0.04)$ corresponding to the two dark spots in figure 5. The lines are just guides for the eyes and connect values for O sites or the other sites. Bottom: fraction of s, p and d symmetry in $n(E_F, k_{\parallel})$ for these two k_{\parallel} vectors on each inequivalent layer of the Co/SrTiO₃ multilayer.

seems to be general and has also been found in the conductance distributions [14]. This can be understood in terms of the interfacial Co DOS at the Fermi level (figures 2 and 4):

- (i) the majority spin DOS has nearly no states available for propagating evanescently into the oxide layer, whereas
- (ii) the minority spin DOS has a large number of states, corresponding mainly to d states, that hybridize strongly with the SrO states (see figure 2) and give rise to a large number of evanescent wavefunctions whose k_{\parallel} vectors correspond to the continuous line in figure 5.

In our multilayer geometry, corresponding to thin Co layers separated by insulating layers, quantum well states can occur and fortuitously even couple to the evanescent states if their k_{\parallel} coincide. This has not to occur because these quantum well states have no physical reality and result only from the particular superlattice construction. A careful comparison of the band

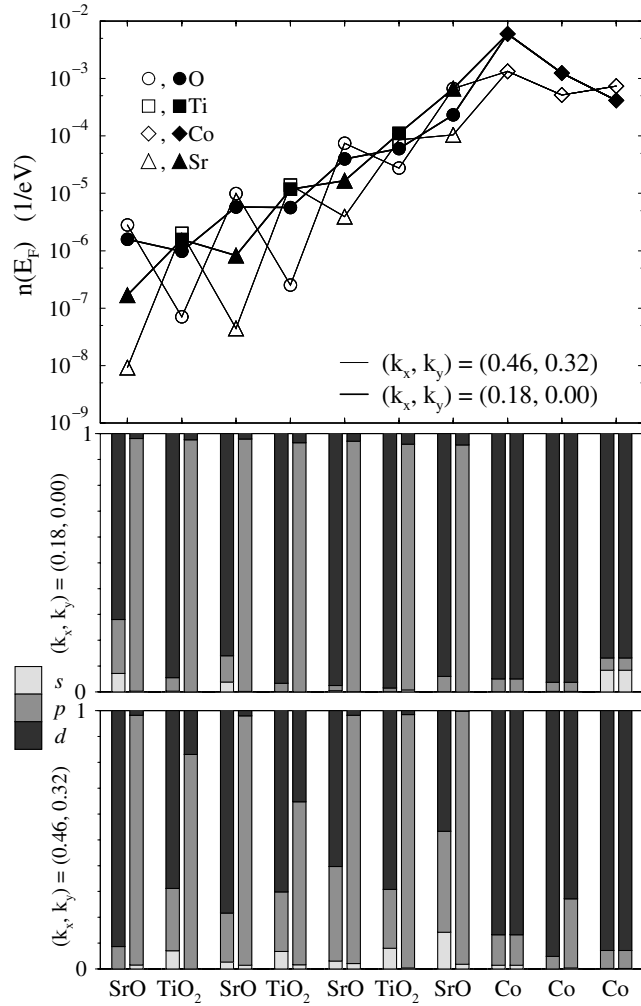


Figure 7. Top: k_{\parallel} projected minority spin density of states values $n^{\downarrow}(E_F, k_{\parallel})$ at the Fermi level E_F on each inequivalent layer of the Co/SrTiO₃ multilayer for $(k_x, k_y) = (0.18, 0.00)$ and $(0.46, 0.32)$ corresponding to the two dark spots in figure 5. The lines are just guides for the eyes and connect values for O sites or the other sites. Bottom: fraction of s, p and d symmetry in $n(E_F, k_{\parallel})$ for these two k_{\parallel} vectors on each inequivalent layer of the Co/SrTiO₃ multilayer.

structures between bulk Co and the present central Co layer along high symmetry lines of the two-dimensional Brillouin zone does not show clear evidence of the occurrence of such quantum well states (or they remain at a negligible level). Moreover, the high values spots for majority spin of figure 5 do not correspond to resonances into the DOS of the Co layer, indicating that the processes which select k_{\parallel} vectors of the evanescent states originate well inside the oxide. This allows us to assume that the quantum well states present in the Co layer do not significantly affect the tunnelling states.

Let us now focus on the decay of the Fermi level states for the two highest k_{\parallel} -states in figure 5 for each spin: $(k_x, k_y) = (0.34, 0.12)$ and $(0.20, 0.04)$ for majority spin (figure 6) and $(k_x, k_y) = (0.18, 0.00)$ and $(0.46, 0.32)$ for minority spin (figure 7). The decay of $n(E_F)$

into the oxide layer corresponds to the decay of the evanescent wavefunctions at E_F . As expected, this decay depends exponentially with the distance to the Co/SrO interface and has a modulation related to the chemical nature of the site. The minority spin states decay faster into the oxide than the majority ones but, because a large number of k_{\parallel} -states will contribute to the conductivity, it is not possible to conclude that the minority spin channel conducts less than the other spin channel for the present oxide thickness. However, we can conclude that for large enough oxide thickness, the majority spin channel will become dominant, and the induced total polarization \tilde{P} will change sign and become positive. The s, p and d fraction of $n(E_F)$ is also given in figures 6 and 7, allowing us to discuss the relative decay for each symmetry. As expected, the O sites carry nearly only p states, and the Sr and Ti sites carry mainly d states. However, for the majority spin states, where the Co carry a low level of d states than for the minority ones, the d states are less present on the Ti sites and even become small on the Sr sites (see figure 6 for $(k_x, k_y) = (0.20, 0.04)$).

For the discussion of the result of De Teresa *et al* [2], particularly essential is the decay of these tunnelling d states wavefunctions because they are expected to overlap with the electrode magnetic d states more than tunnelling s or p ones. The present work shows that d state induced wavefunctions into the SrTiO₃ oxide layer do not decay more rapidly than s or p ones due to the high d character of the DOS on Ti and Sr sites. Consequently, we conclude that the oxide induced polarization \tilde{P} , mainly mediated by the Sr and Ti atoms, is dominated by d states, making the Co/SrTiO₃ system well suited for studying the role of a direct interaction of the spin polarized tunnelling current and the magnetic electrodes. Open questions remain, and these are mainly on the transferability of these conclusions to other kinds of oxide (such as Al₂O₃ and MgO) for which s states are supposed mainly to carry the polarization.

From this study, we finally conclude that it is difficult to discuss the polarization P_i of a given electrode needed by expression (1) when we only have access to \tilde{P}_i (which is a crude approximation of P_i for electrode i) or to the polarization \tilde{P} of the evanescent states into the oxide layer which results from the superposition of states from both electrodes. This restricts the use of Jullière's expression to the determination of effective electrode polarizations P_i which can hardly be related to band structure quantities without calculating the magneto-conductivity explicitly.

References

- [1] Moodera J S *et al* 1995 *Phys. Rev. Lett.* **74** 3273
- [2] De Teresa J M *et al* 1999 *Phys. Rev. Lett.* **82** 4288
- [3] Bardou F 1997 *Europhys. Lett.* **39** 239
- [4] Da Costa V *et al* 1999 *Eur. Phys. J. B* **13** 297
- [5] Tiusan C *et al* 2001 *Phys. Rev. B* **64** 104423
- [6] Faure-Vincent J *et al* 2002 *Phys. Rev. Lett.* **89** 107206
- [7] Butler W H *et al* 2001 *Phys. Rev. B* **63** 054416
- [8] Oleinik I I *et al* 2001 *Phys. Rev. B* **65** 020401(R)
- [9] Jullière M 1975 *Phys. Lett. A* **54** 225
- [10] Mavropoulos Ph, Papanikolaou N and Dederichs P H 2000 *Phys. Rev. Lett.* **85** 1088
- [11] Williams A R *et al* 1979 *Phys. Rev. B* **19** 6094
- [12] van Benthem K, Elsässer C and French R H 2001 *J. Appl. Phys.* **90** 6156
- [13] Montaigne F, Hehn M and Schuhl A 2001 *Phys. Rev. B* **64** 144402
Xiang X H *et al* 2002 *Phys. Rev. B* **66** 174407
- [14] Butler W H *et al* 2001 *Phys. Rev. B* **63** 054416